Electronic Supplementary Material (ESI) for Physical Chemistry Chemical Physics.

Spectroscopic and Photophysical Study of the Demetallation of a Zinc Porphyrin and the Aggregation of its Free Base in a Tetraalkylphosphonium Ionic Liquid

Neeraj K. Giri, Abhinandan Banerjee, Robert W. J. Scott, Matthew F. Paige,* and Ronald P. Steer*

Supporting Information

1. Purification of the ionic liquid

A 25 mL aliquot of the ionic liquid was dissolved in 50 mL of dichloromethane and *ca.* 1g activated charcoal added. The mixture was stirred overnight and filtered to recover a clear solution of the ionic liquid in dichloromethane. A specially prepared column, similar to the ones used by Earle, *et al.*[1] for alkylimidazolium ionic liquid purification, was then used for the subsequent purification steps. The column itself was an ordinary one used in conventional chromatography, with a 24/40 female joint on top. It contained Celite on the bottom, flash chromatographic silica gel in the middle, and alumina on top; it was expected that passage through this column would remove all charged contaminants from the ionic liquid solution.

The column was subjected to a pretreatment step with *ca*. 100 mL dichloromethane prior to its use. Then the filtrate from the previous step was passed through the column, and finally, another 50 mL dichloromethane was used to elute the remainder of the ionic liquid. A Schlenk adapter was used in order to create a higher superincumbent pressure of gaseous nitrogen over the column, which accelerated the rate of flow of the liquid through the column.

Once eluted, the neat ionic liquid was obtained from the eluate by heating it at 55°C in vacuo. ^{1}H NMR spectroscopy of the purified ionic liquid in $CDCl_3$ failed to suggest the presence of any impurities (*cf*. Figure S1, below).

1. Earle, M. J.; Gordon, C. M.; Plechkova, N. V.; Seddon, K. R.; Welton, T., *Anal. Chem.* **2007**, *79*, 758–764.

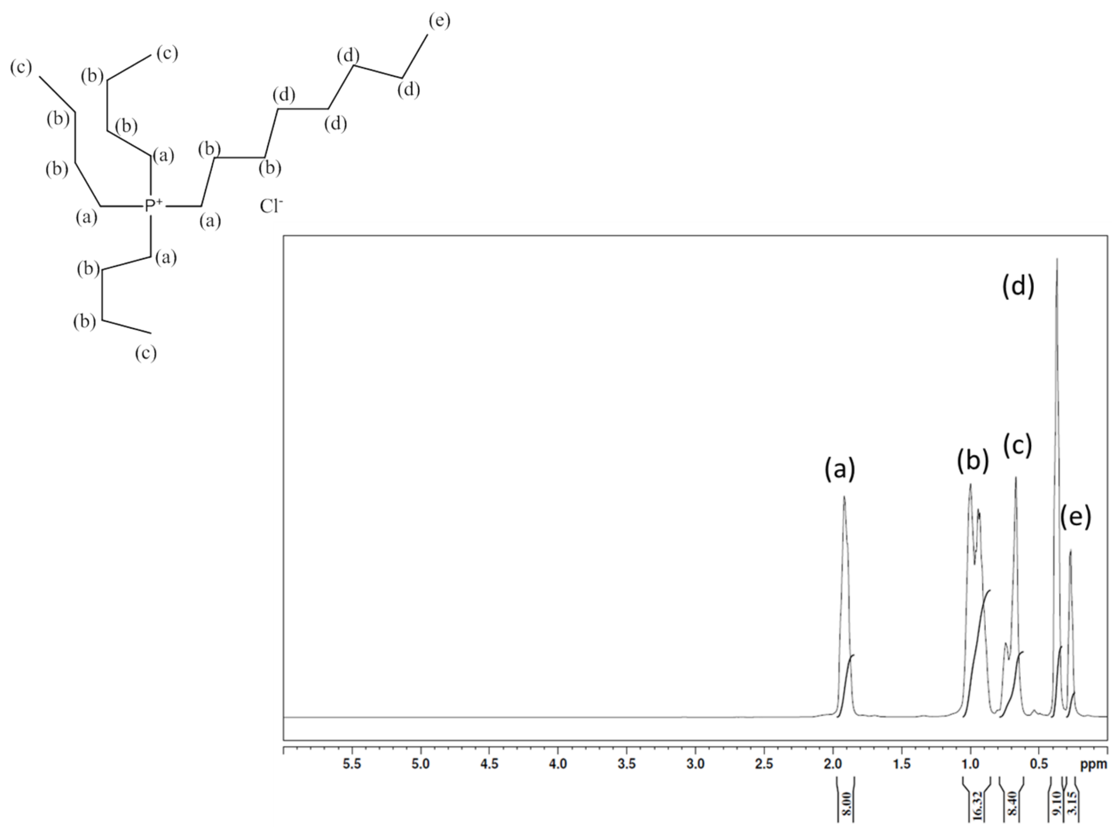

Figure S1: ^{1}H NMR spectrum of the P4448Cl ionic liquid in $CDCl_3$.

2. Derivation of the relationships between modelled Gaussian areas of the absorption spectra on a cm^{-1} ($\bar{\nu}$) scale, the concentrations of the species present in the system and the thermodynamics of the aggregation equilibrium.

Mass balance: $[M] + 2[J] = \text{constant}$ for only dimeric aggregates

At equilibrium: $2\,M \rightleftharpoons J$; $K_{eq} = [J]/[M]^2$, using activity = molar concentration

From the Beer-Lambert Law: $\text{Absorbance}(\bar{\nu}) \propto \varepsilon(\bar{\nu})c$, where c is the molar conc.

$A = \text{Area of Gaussian} \propto \int \text{Absorbance}(\bar{\nu}) \propto c\int\varepsilon(\bar{\nu})$

$\int\varepsilon(\bar{\nu}) \propto f$, the oscillator strength of the transition

$A/f \propto$ concentration; $A_M/f_M \propto [M]$ and $A_J/f_J \propto [J]$

So, using a common proportionality constant, C:
$CA_M/f_M = [M]$ and $CA_J/f_J = [J]$

$$K_{eq} = [J]/[M]^2 = (CA_J/f_J)/(CA_M/f_M)^2 = \{f_M{}^2/(Cf_J)\}\{A_J/(A_M)^2\}$$

$$f_J = \beta f_M \quad \text{where } 2.0 \le \beta = f_J/f_M \le 1.0 \text{ if } n = 2$$

$$A_J/(A_M)^2 = \{Cf_J/(f_M)^2\}K_{eq} = (K_{eq})\{C\beta/f_M)\}$$

Van't Hoff equation: $\ell n\{K_{eq}\} = -\Delta G°/(RT)$ and $d\{\ell n(K_{eq})\}/d\{1/T\} = -\Delta H°/R$

$$\ell n\{A_J/(A_M)^2\} = \ell n\{K_{eq}\} + \ell n\{C\beta/f_M)\}$$

If $(C\beta/f_M) \neq f(T)$, then the slope of a graph of $\ell n\{A_J/(A_M)^2\}$ vs. $1/T$ will give a slope = $-\Delta H°/R$, from which $\Delta H°$ for the equilibrium reaction can be obtained.

Mass Balance: $2[J] + [M]$ = constant at all temperatures (if only dimerization)

$2CA_J/f_J + CA_M/f_M$ = constant at all temperatures

$(2f_M/f_J)A_J + A_M$ = (constant)(f_M/C) = constant'

$2A_J/\beta + A_M$ = constant'

Do trials for allowed values of β: $2.0 \le \beta = f_J/f_M \le 1.0$ (*cf.* Table S1). Use A1 for A_J and the sum of A3+A4+A5 (B(0,0) + B(1,1) + B(1,0)) for A_M. The best fit is for $\beta \sim 2$, suggesting that the J dimers are primarily in a side-by-side arrangement.

3. Modelling of absorption spectra (on a cm^{-1} scale) by a sum of Gaussian features; xc_i are the peak wavenumbers, w_i are the FWHM, A_i are the areas

a. 2.5 μM H_2TPP in IL; the Soret region, Figure S2 and Table S1

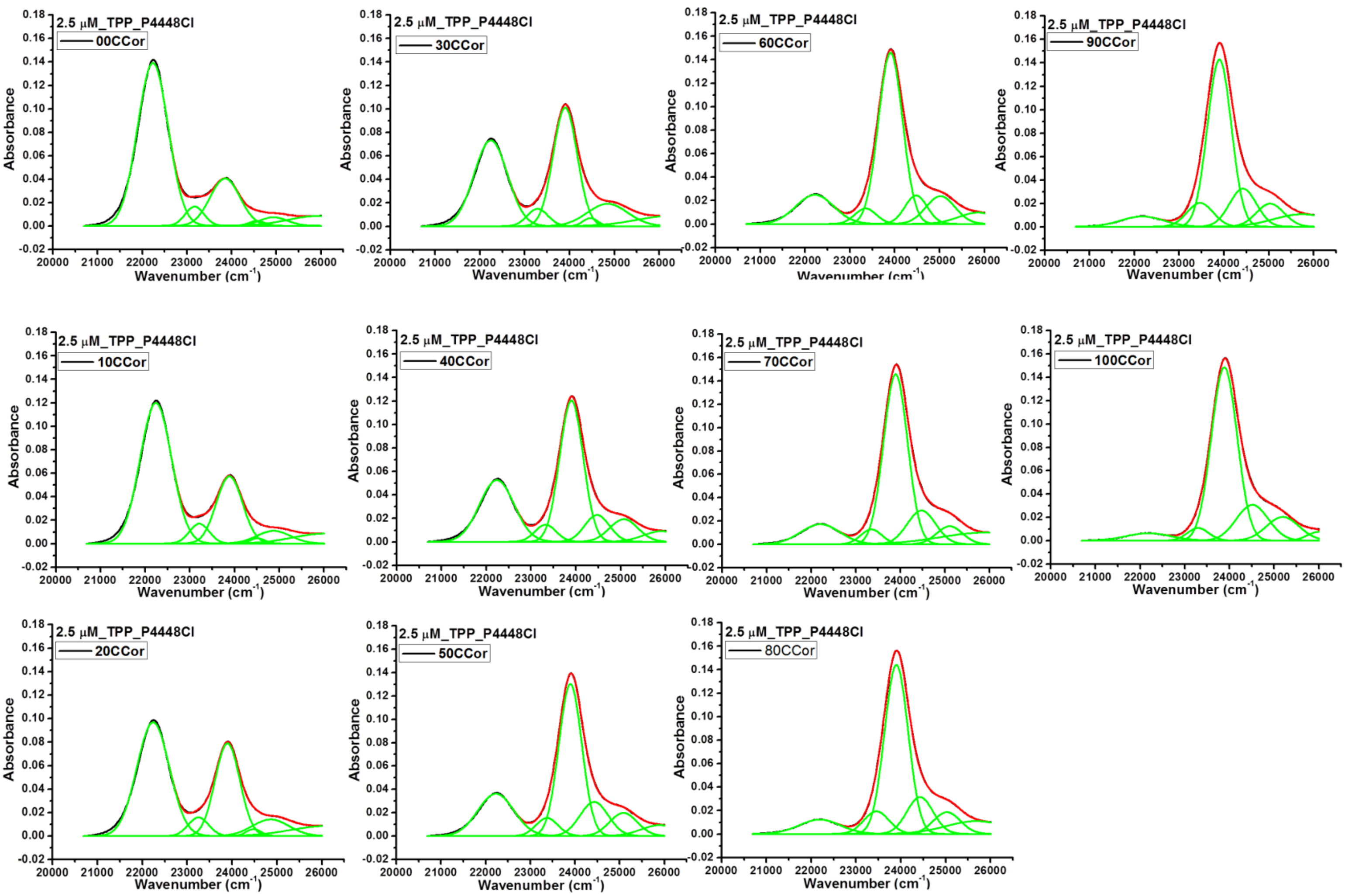

Figure S2: Modelling of absorption spectra at ten degree intervals; the Soret region for 2.5 μM H_2TPP in the P4448Cl IL. A sixth Gaussian centered at 24565 cm^{-1} has been inserted between B(0,0) and B(1,0) to account for hot bands (see text).

Table S1: Modelling of Soret absorption spectra (on a cm^{-1} scale) by a sum of Gaussian features for 2.5 μM H_2TPP in P4448Cl IL at ten degree intervals. The xc_i are the peak wavenumbers, w_i are the FWHM, A_i are the areas.

P	0°C	10°C	20°C	30°C	40°C	50°C	60°C	70°C	80°C	90°C	100°C
Chi^2/DoF	2.8411E-6	2.2562E-6	1.6361E-6	1.0503E-6	6.4028E-7	3.2707E-7	1.7992E-7	1.1024 E-7	4.9378E-8	3.8556E-8	9.3196E-8
R^2	0.9982	0.9981	0.9981	0.9987	0.9993	0.9997	0.9998	0.9999	0.9999	0.99998	0.9999
y0	0	0	0	0	0	0	0	0	0	0	0
xc1	22237±1	22239±2	22241±2	22241±2	22236±2	22228±2	22216±2	22201±10	22186 ±3	22176 ±4	22185±9
w1	688±3	704±3	724±4	746±4	773±4	807±5	848±5	887±13	923 ±7	964 ±9	1014 ±19
A1	120±0.4	106±0.4	87.9±0.4	68.5±0.3	51.0±0.2	36.7±0.2	26.4 ±0.1	19.16±0.48	14.14 ±0.09	10.61±0.09	8.12±0.13
xc2	23171 ±26	23212±32	23250±33	23287±36	23323±58	23372±71	23348±46	23349±46	23456 ±78	23468±85	23295±37
w2	426 +42	447 ±43	458 ±45	468 ±44	478 ±54	497 ±55	482 ±34	482 ±52	565 ±46	585 ±49	489 ±31
A2	8.8 ±1.8	9.5 ±1.9	9.15 ±2.03	8.71 ±1.70	8.73 ±2.62	9.66 ±3.45	8.01 ±2.01	7.76 ±3.04	13.66 ±4.89	14.96 ±5.68	6.69 ±1.47
xc3	23853±28	23885±35	23898±21	23903±17	23901±20	23896±25	23906±5	23893 ±10	23902 ±8	23900 ±8	23885 ±16
w3	671 ±60	587 ±62	552 ±27	537 ±24	525 ±36	514 ±35	539 ±18	538 ±18	527 ±20	532 ±20	576 ±19
A3	34±5.3	42±6	55±4	68±8.3	79.2 ±11.7	83.8 ±22.6	98.7 ±5.3	98.2 ±9.3	95.2 ±12.9	95.2 ±13.7	107.2 ±15
xc4	24561±177	24511±59	24479±44	24462±33	24473±111	24429±91	24476±36	24475±50	24429 ±40	24426±37	24514±196
w4	367±539	339±381	338±220	334±147	556±372	634 ±587	501 ±105	642±227	588 ±156	603±172	721±543
A4	1.92±13.64	1.91±9.13	2.51±6.62	2.89±5.18	15.9±26.0	23.3 ±39.1	15.26±10.51	23.27±15.59	23.18±10.14	24.66±12.72	27.78±45.98
xc5	24934±728	24876±278	24859±167	24848±259	25069±181	25083±215	25020±56	25105±106	25028 ±109	25032±109	25194±491
w5	638±2298	761±2028	826±1798	908±1237	639±589	625 ±460	654±250	586±103	605±186	622±188	740±551
A5	5.82±60	10.33±82	14.7±111.1	21.8±91.1	15.4±29.83	15.6±31.0	19.44 16.27	11.39±7.56	14.11±18.23	15.39±18.74	18.91±36.11
xc6	25950±587	26004±814	26103±1269	26313±4995	25903±413	25888±380	25855±300	25927±347	25684 ±699	25743±551	25999±66
w6	1385±9287	1405±11734	1609±19975	1603±19404	803±1279	837 ±1084	882 ±775	2058±2013	1368 ±1490	1278±1254	522±200
A6	14.7±101.5	14.9±131.9	17.2±226.9	18.10±250.7	9.1±18.2	9.74±15.88	10.67±11.96	26.05±25.85	18.65 ±25.51	17.02±20.73	5.02±4.13

b. 2.5 μM ZnTPP in IL; the Soret region, Figure S3 and Table S2

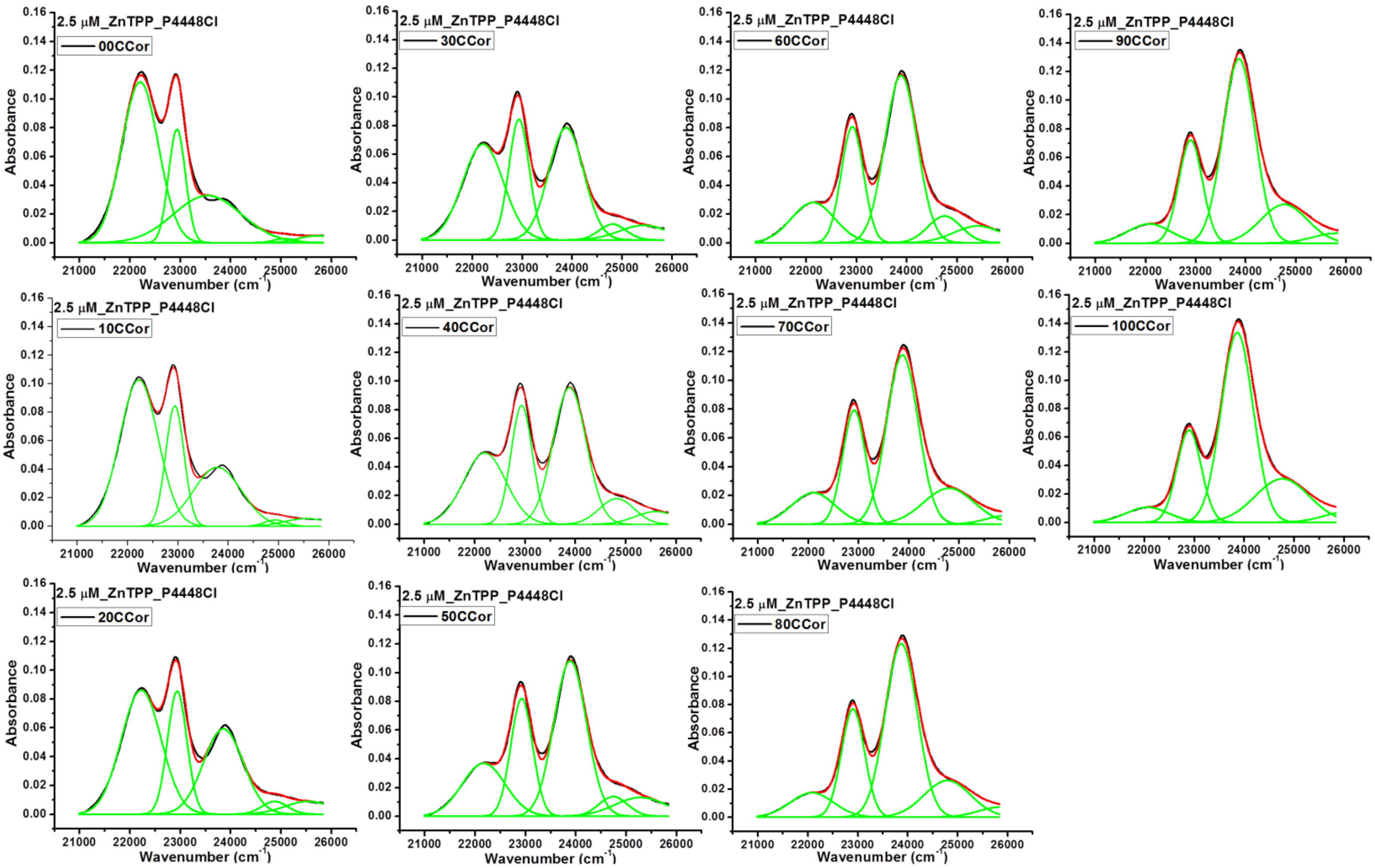

Figure S3: Modelling of absorption spectra at ten degree intervals; the Soret region for 2.5 μM ZnTPP in the P4448Cl IL prior to completion of the demetallation (see text).

Table S2: Gaussian modelling of Soret absorption bands for 2.5 μM ZnTPP in the P4448Cl IL prior to complete demetallation.

P	0°C	10°C	20°C	30°C	40°C	50°C	60°C	70°C	80°C	90°C	100°C
Chi^2 /DoF	2.4067E-6	2.5784E-6	2.7048E-6	2.6383E-6	2.4062E-6	2.1439E-6	1.9227E-6	1.7515E-6	1.5312E-6	1.2721E-6	1.0962E-6
R^2	0.99859	0.99813	0.99741	0.99699	0.99728	0.99783	0.99827	0.99856	0.99884	0.99913	0.99933
y0	0	0	0	0	0	0	0	0	0	0	0
xc1	22202 ±4	22221 ±3	22223 ±5	22214 ±7	22197 ±9	22169 ±11	22135 ±14	22100 ±16	22083 ±18	22071 ±22	22057 ±26
w1	730 ±6	762 ±6	792 ±8	817 ±11	842 ±15	859 ±19	866 ±24	861 ±28	869 ±33	864 ±39	853 ±46
A1	102 ±2	98 ±1	86 ±1	69 ±1	53 ±1	40 ±1	30 ±1	24 ±1	19 ±1	15 ±1	11 ±1
xc2	22934 ±2	22936 ±2	22938 ±2	22936 ±3	22931 ±3	22924 ±2	22917 ±2	22911 ±2	22905 ±2	22901 ±2	22897 ±2
w2	337 ±5	366 ±5	387 ±5	407 ±6	422 ±6	434 ±6	444 ±6	456 ±5	462 ±5	472 ±6	485 ±6
A2	33 ±1	39 ±1	41 ±1	43 ±1	44 ±1	45 ±1	45 ±1	45 ±1	45 ±1	43 ±1	39 ±1
xc3	23539 ±37	23782 ±10	23856 ±6	23880 ±7	23884 ±8	23888 ±9	23886 ±5	23872 ±9	23871 ±10	23866 ±9	23859 ±7
w3	1355 ±71	953 ±36	793 ±16	703 ±12	659 ±13	647 ±10	643 ±9	629 ±12	640 ±11	640 ±11	639 ±12
A3	56 ±3	50 ±2	59 ±1	69 ±2	79 ±2	88 ±4	94 ±2	93 ±7	99 ±6	103 ±6	107 ±9
xc4	25068 ±303	24936 ±102	24873 ±93	24808 ±69	24823 ±195	24740 ±33	24750 ±134	24796 ±91	24794 ±167	24766 ±244	24761 ±89
w4	442 ±448	447 ±362	515 ±236	544 ±256	693 ±252	575 ±289	663 ±245	1012 ±445	936 ±438	936 ±499	1082 ±480
A4	2 ±6	3 ±7	6 ±11	8 ±15	16 ±15	10 ±24	16 ±26	32 ±17	31 ±21	32 ±30	42 ±23
xc5	25710 ±225	25546 ±503	25534 ±427	25425 ±643	25600 ±523	25282 ±857	25407 ±851	25946 ±475	25841 ±412	25806 ±822	26059 ±846
w5	737 ±1653	882 ±1478	922 ±1144	977 ±1149	825 ±1028	1033 ±1066	964 ±1119	810 ±1907	864 ±1743	940 ±2436	924 ±2648
A5	5 ±10	6 ±11	10 ±15	13 ±19	9 ±17	17 ±29	14 ±28	6 ±22	8 ±24	8 ±32	9 ±38

4. Figure S4: Van't Hoff plot for 25μM porphyrin in P4448Cl ionic liquid

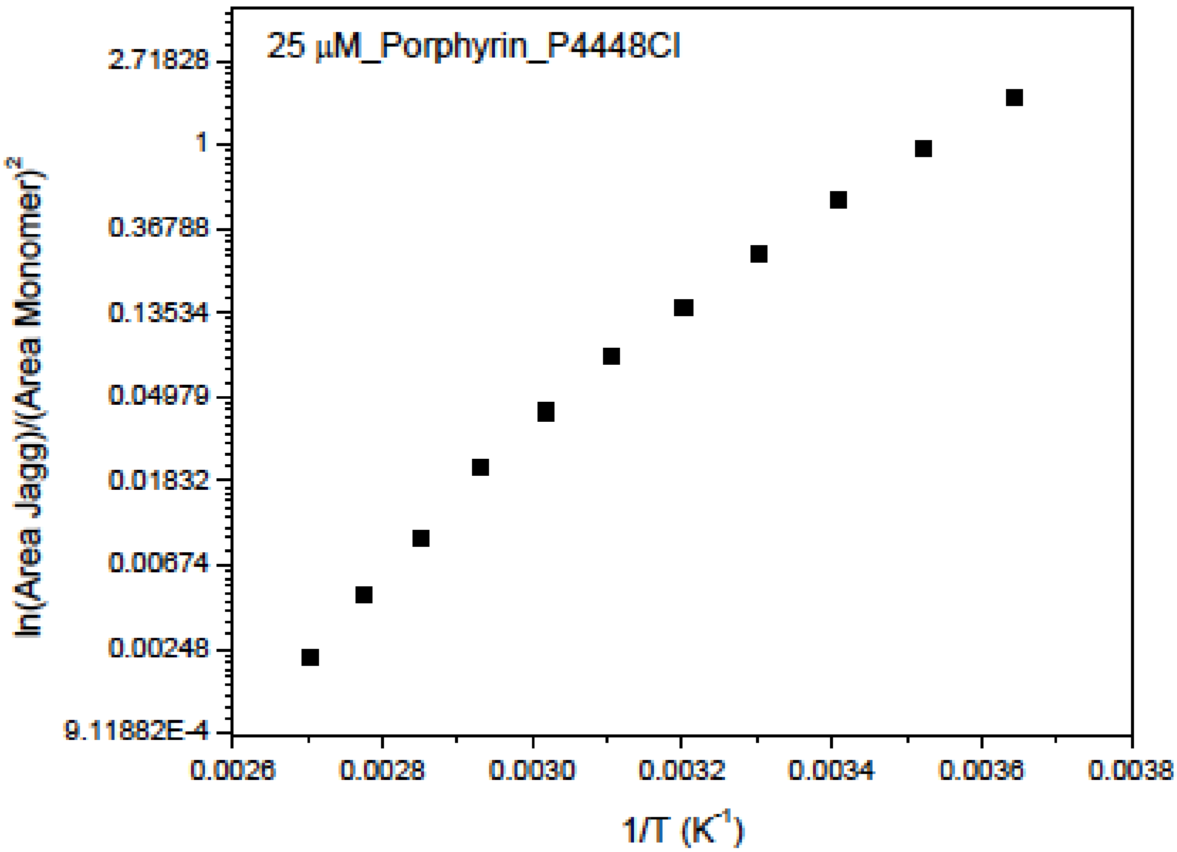

5. Modelling of Q band absorption spectra (on a cm^{-1} scale) by a sum of Gaussian features; xc_i are the peak wavenumbers, w_i are the FWHM, A_i are the areas

2.5 μM H_2TPP in IL; the Q band region, Figure S5 and Table S3

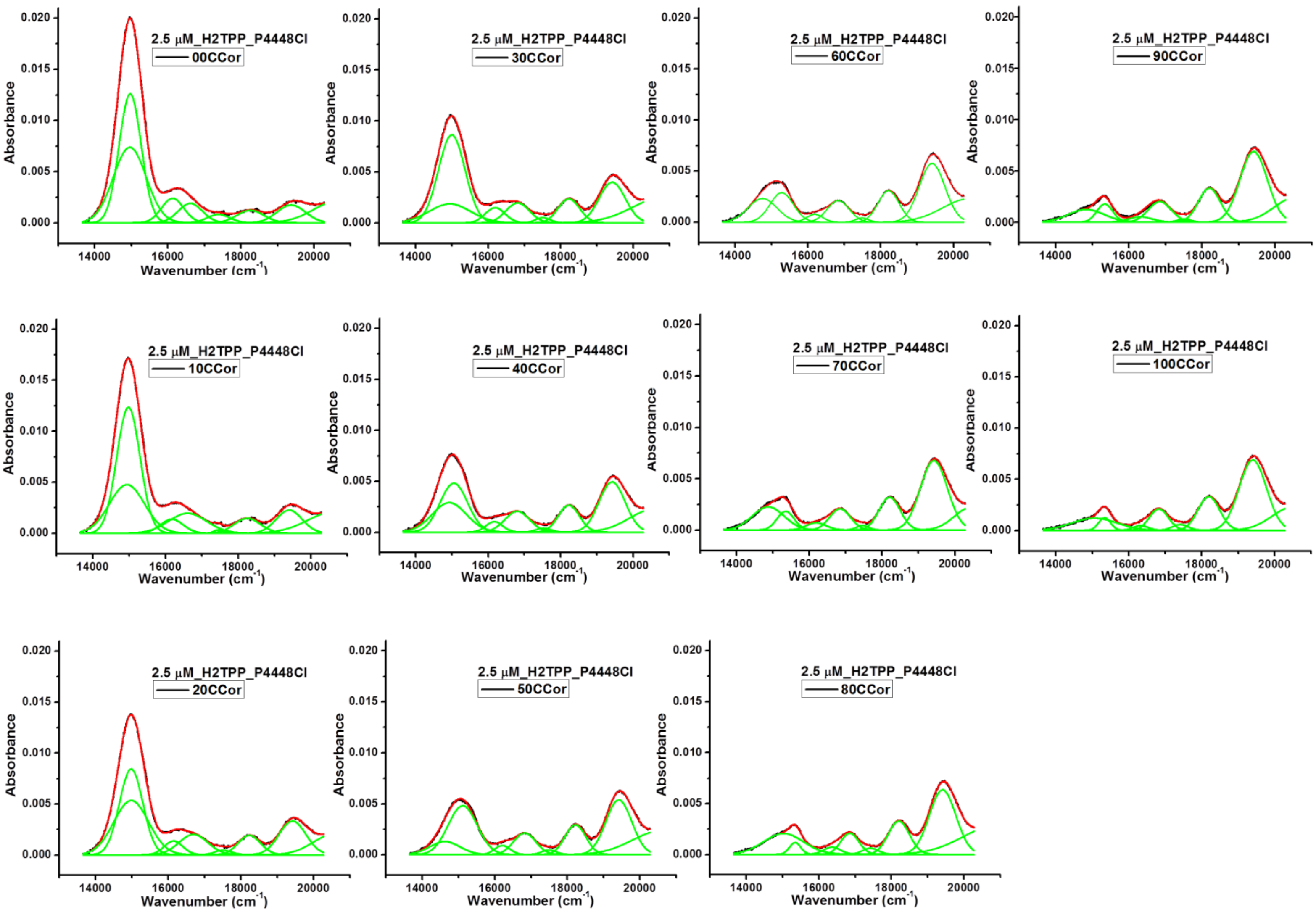

Figure S5: Modelling of absorption spectra at ten degree intervals; the Q band region for 2.5 μM H_2TPP in the P4448Cl IL.

Table S3: Modelling of absorption spectra (on a cm^{-1} scale) in the Q band region at ten degree intervals by a sum of Gaussian features for 2.5 μM H_2TPP in P4448Cl IL. The xc_i are the peak wavenumbers, w_i are the FWHM, A_i are the areas.

P	0°C	10°C	20°C	30°C	40°C	50°C	60°C	70°C	80°C	90°C	100°C
Chi^2 /DoF	4.5647E-9	4.3258E-9	4.5787E-9	5.4898E-9	7.1832E-9	8.8878E-9	8.2527E-9	5.908E-9	3.7977E-9	7.2827E-9	3.8049E-9
R^2	0.99985	0.9998	0.99967	0.99929	0.99835	0.99693	0.99671	0.99768	0.99857	0.99743	0.99871
y0	0	0	0	0	0	0	0	0	0	0	0
xc1	14967±3	14978±9	14980±2	15000±5	14926±123	14621±536	14753±81	14873±33	15026±9	14831±48	15.57±14
w1	604±9	642±14	645±12	733±15	950±43	835±250	791±57	876±31	1107±10	986±53	1245±17
A1	9.5±0.8	9.9±1.4	6.8±12	7.9±0.7	3.4±2.9	1.4±2.7	2.3±0.5	2.5±0.2	2.9±0.0	1.5±0.1	1.9±0.0
xc2	14957±12	14937±96	14982±6	14942±56	15053±16	15116±120	15281±33	15352±5	15348±3	15342±5	15339±3
w2	902±14	970±36	960±24	1158±60	759±65	799±63	644±33	476±22	312±9	438±18	331±8
A2	8.3±0.8	5.8±1.9	6±0.7	2.7±0.8	4.6±2.9	4.8±2.7	2.3±0.5	1.1±0.2	0.5±0.0	0.9±0.1	0.5±0.0
xc3	16130±272	16168±31	16143±44	16194±52	16168±27	16206±33	16190±31	16190±64	16361±107	16311±616	16321±90
w3	613±170	633±247	520±78	551±68	461±50	438±48	447±51	557±92	475±95	646±437	422±88
A3	1.8±3.0	1.1±2.7	0.9±0.7	1.0±0.4	0.6±0.2	0.5±0.1	0.4±0.1	0.5±0.1	0.4±0.2	0.4±1.0	0.3±0.2
xc4	16614±438	16603±659	16692±126	16816±50	16802±21	16823±14	16835±12	16848±19	16854±27	16844±149	16825±16
w4	665±533	1058±624	798±247	656±116	685±77	616±68	610±47	574±47	501±81	634±155	522±77
A4	1.6±3.4	2.6±3.4	2.0±0.9	1.6±0.4	1.8±0.2	1.6±0.2	1.6±0.1	1.5±0.2	1.3±0.3	1.6±1.0	1.4±0.3
xc5	17381±149	17448±12.8	17507±52	17503±36	17517±39	17489±44	17489±30	17459±24	17417±59	17502±45	17405±65
w5	620±241	254±43	461±111	415±76	400±90	410±93	356±65	344±46	438±82	359±92	449±87
A5	0.6±0.6	0.1±0.04	0.3±0.2	0.3±0.1	0.2±0.1	0.2±0.1	0.2±0.1	0.2±0.0	0.3±0.1	0.1±0.1	0.3±0.1
xc6	18259±30	732±85	18231±7	18226±13	18229±12	18223±10	18216±9	18210±3	18205±6	18200±3	18195±3
w6	740±100	732±85	618±22	599±34	582±27	575±	580±20	582±8	584±17	597±10	598±8
A6	1.1±0.2	1.3±0.4	1.5±0.1	1.8±0.2	1.9±0.2	2.1±0.2	2.2±0.2	2.3±0.0	2.4±0.1	2.5±0.0	2.5±0.0
xc7	19375±115	19402±43	19421±49	19419±7	19422±35	19418±7	19411±6	19426±20	19411±4	19409±28	19400±21
w7	780±193	719±203	740±51	723±60	721±107	715±45	709±41	741±18	732±26	748±29	750±23
A7	1.7±1.9	2.0±2.8	3.1±1.0	3.6±1.1	4.5±3.2	4.8±1.1	5.1±1.1	6.2±0.5	5.8±0.7	6.5±1.2	6.5±1.0
xc8	20664±1239	20666±1850	20569±594	20861±773	20578±1065	20609±305	20468±211	20445±160	20878±405	20556±560	20519±351
w8	1351±2660	1496±4380	1165±1380	1768±1629	1368±3483	1648±940	1529±729	914±442	1863±853	1172±1355	1181±1031
A8	3.6±9.3	4.0±14.5	2.9±4.5	5.7±6.5	3.9±11.5	4.9±2.9	4.7±2.2	2.5±1.6	6.5±3.6	3.6±5.2	3.4±3.6

6. Absorption spectra of the purified ionic liquid as a function of temperature

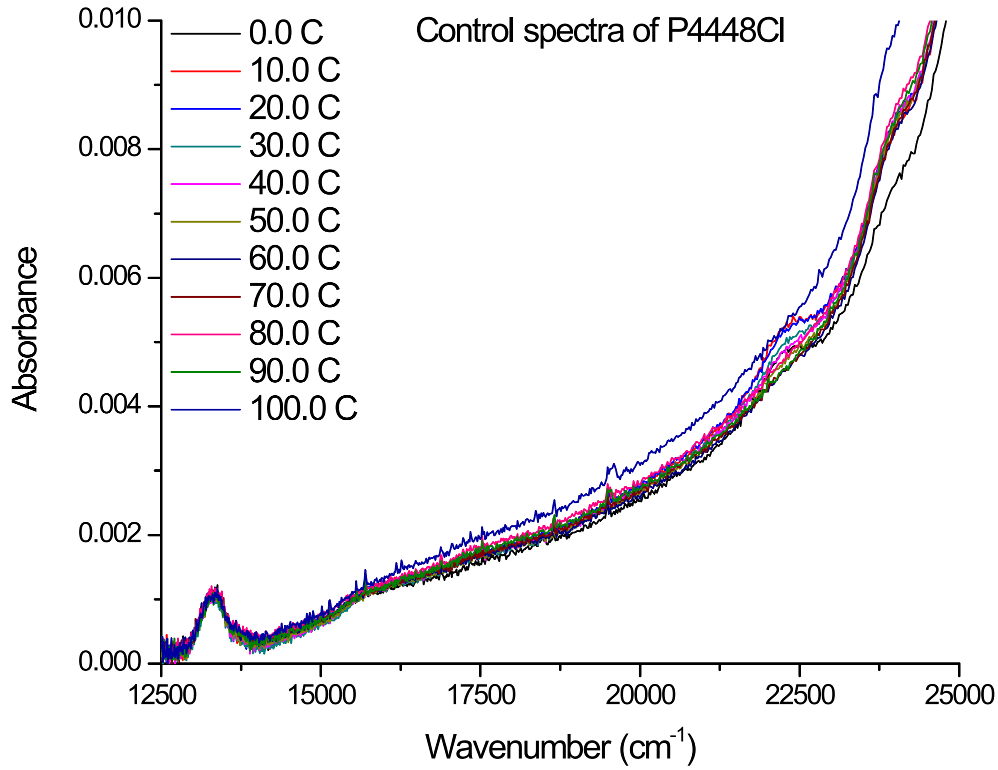

Figure S6: Absorption spectrum of control P4448Cl ionic liquid. Measurements are performed under the same experimental conditions as reported for samples. The absorption band at 13300 cm^{-1} is the $\Delta v = 5$ C–H stretching overtone of the alkyl substituents of the IL.[2]

2. Henry, B. R.; Greenlay, W. R. A., *J. Chem. Phys.* **1980**, *72*, 5516-5524.

7. Fluorescence decay profiles: 2.5 μM H_2TPP in undegassed P4448Cl ionic liquid at room temperature. Log_{10}(total counts) vs. time in ns. The solid line is the multiexponential fit. The bottom panel is the distribution of weighted residuals. The green curve is the instrument response function. The full set of data extracted from these decays is in Table 1 of the main text.

Figure S7A: Excitation in Soret J aggregate band at 458 nm, observation at 693 nm

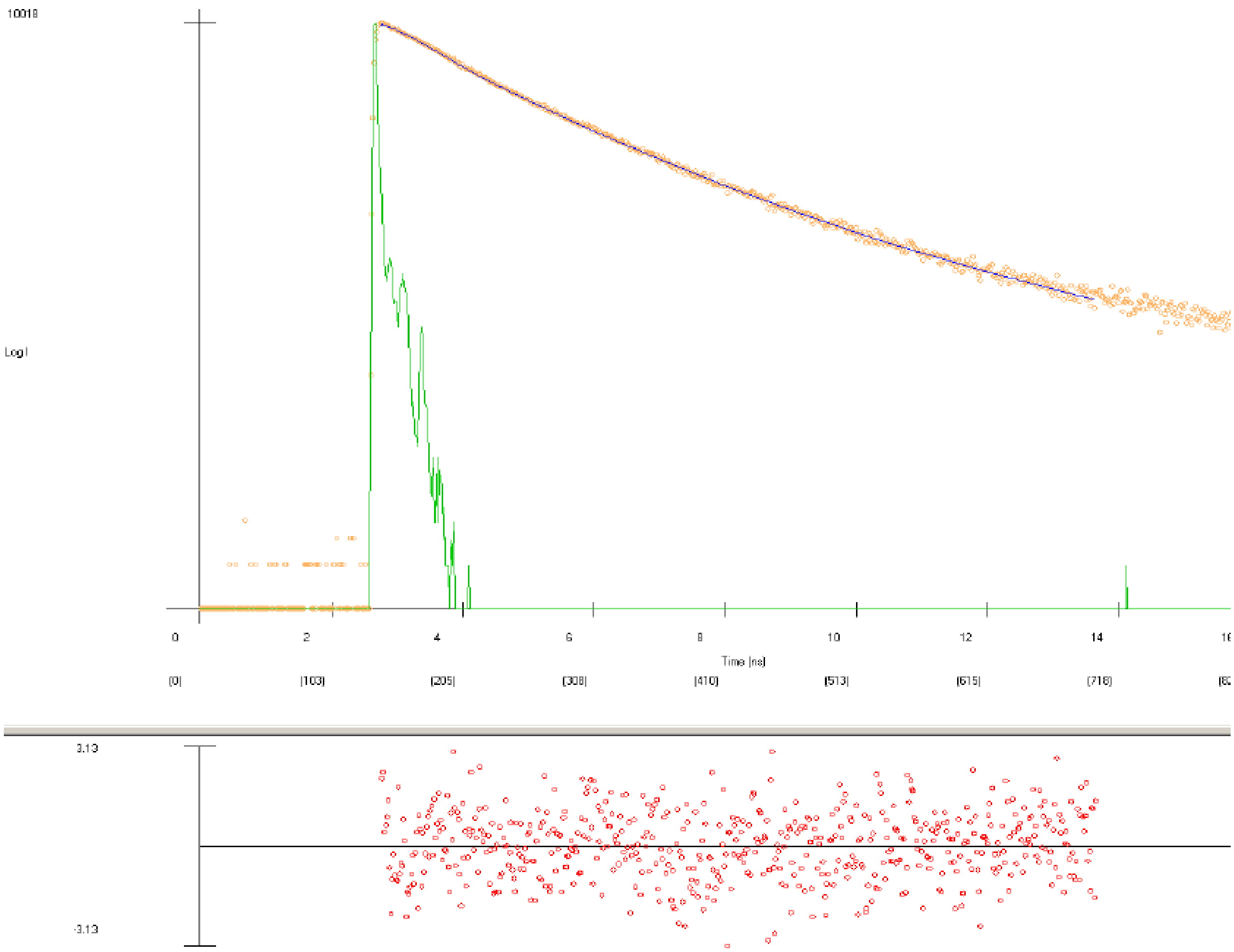

Figure S7B: Excitation in Soret monomer band at 414 nm, observation at 716 nm

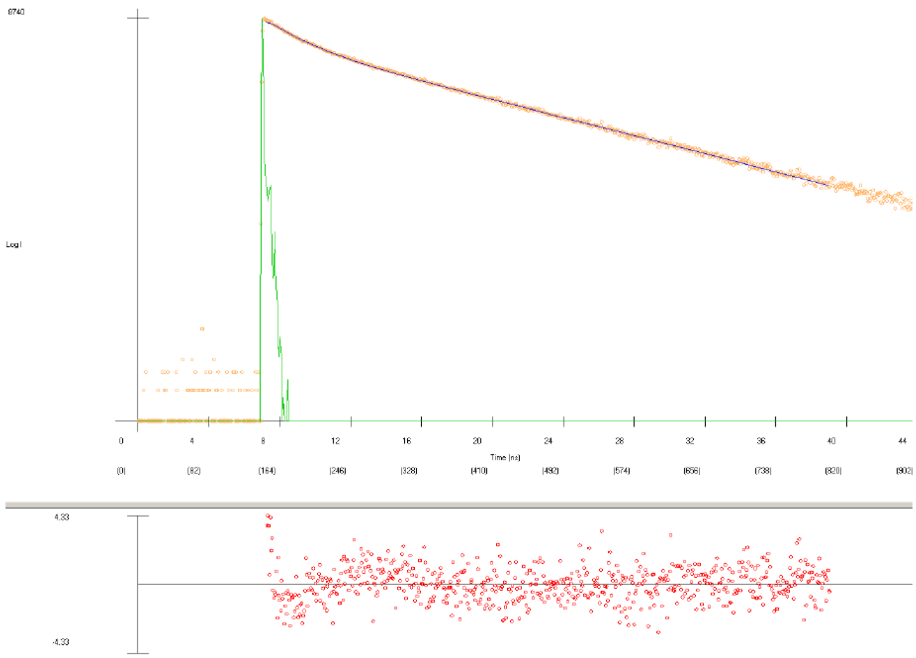

Figure S7C: Excitation in the Soret monomer/J dimer overlap region at 436 nm, observation at 693 nm